THE UNIVERSITY OF CHICAGO

The Enrico Fermi Institute

Semi-Annual Report

to

The National Aeronautics and Space Administration

on work under Grant No. NSG-2057

For the period: 1 June 1982 to 1 December 1982

FAR INFRARED AND SUBMILLIMETER ASTRONOMY WITH THE GERARD P. KUIPER AIRBORNE OBSERVATORY

Roger H. Hildebrand
Principal Investigator

FAR-INFRARED AND SUBMILLIMETER ASTRONOMY WITH THE GERARD P. KUIPER AIRBORNE OBSERVATORY

I. INSTRUMENTATION

As the first steps in building a submillimeter polarimeter (to be described in the next report), we have built a rail system to help install the instrument at the focal plane, and we have developed a high-quality spectral filter giving $\Delta\lambda/\lambda = 16\%$ at 300 μm.

A. Rail System

To avoid noise from diffracted radiation reflected in the air bearing, the various groups doing far-IR and submillimeter photometry have moved their instruments to an almost inaccessible position inside the instrument flange. Because of the even greater difficulty to be expected when the polarimeter is put in that position, we have built a rail system so that the instrument can be bolted to the beam splitter when the latter is withdrawn from the flange. The polarimeter (or other instrument) and beam splitter can then be easily slid into place as a unit.

This system is proving to be useful to many groups. The design and construction turned out to be much more difficult and expensive than we anticipated. We are pleased with the result but we are having to delay other projects because of the drain on the budget.

B. Spectral Filter

The scientific and instrumental requirements of our polarimetry project have forced us to develop a better spectral filter than has previously been used in submillimeter photometry. The development of a "double half wave" filter (a variety of Fabry-Perot) by graduate student Mark Dragovan has been

very successful. The device is described in Appendix A. Notice particularly the transmission curve shown in Figure 3 of that appendix. The mean wavelength can be varied by changing the spacing of the reflecting grids. The bandwidth can be varied by changing the grid mesh. We will adjust the passband to avoid atmospheric absorption bands.

II. OBSERVATIONS

Our chief advances in observational work have been the completion of the study of a low-mass protostar which we have discovered in a Bok globule and the publication of a paper on the dwarf nova EM Cygni.

A. A Protostar in B335

In flights during the last twelve months we have seen what we believe to be the first direct evidence for a low-mass, pre-main-sequence star in a Bok globule. A manuscript describing this work is presented in Appendix B.

Briefly, we find that more than half of the total far-infrared flux from the globule B335 comes from a region <30 arc sec in diameter approximately centered in the ∿2' × 3' optical image. The far-IR spectrum shows the presence of dust in the core at temperatures well above the mean temperature (∿15 K) of the entire globule. The submillimeter flux density shows a sharp increase in dust column density in the central region. We obtain limits on the luminosity and mass of $<8\ L_\odot$ and $<2\ M_\odot$ for the embedded compact object.

B. EM Cygni

We have made high-speed photometric observations of the dwarf nova EM Cygni at Mt. Semmon. These observations clearly exclude Keplerian orbits as the source of the rapid oscillations. A reprint of the paper describing this work (1982, Stiening, Dragovan, and Hildebrand, P.A.S.P. 94, 642)

accompanies this report. The title and abstract are as follows:

OBSERVATIONS OF THE RAPID OSCILLATIONS OF EM CYGNI

R. F. Stiening, M. Dragovan, and R. H. Hildebrand

We have made high-speed two-color photometric observations of the dwarf nova EM Cyg and have found rapid coherent oscillations with periods between 14.6 and 16.5 seconds. The minimum period is less than the period of a Keplerian orbit at the surface of a carbon white dwarf. The color temperature of the oscillating component is much higher than that of the constant component of the luminosity. These results suggest that the source of the oscillations is the white dwarf or the inner part of the accretion disk.

C. Star Formation in M17SW

A preprint of a paper by Jaffe and Fazio on star formation mechanisms in a giant molecular cloud (1982, Jaffe and Fazio, Ap. J. 257, L77) also accompanies this report.

APPENDIX A

NOTES ON CRYOGENIC METAL MESH BANDPASS FILTERS

M. Dragovan

February 1983

I. INTRODUCTION

We have developed a bandpass filter of the double half wave design for applications in submillimeter astronomy. The principle of the device is discussed briefly in Section III. The design permits tuning to the desired wavelength by changing spacers which are nowhere in contact with the reflecting surfaces (metal mesh reflectors). The width of the passband depends on the grid period of the meshes.[1,2]

Our goal has been to produce a filter with a passband narrow enough ($\Delta\lambda/\lambda \leq 0.2$) for use in a submillimeter polarimeter in which the rotating element is a retardation plate. The width, $\Delta\lambda/\lambda = 0.16$, obtained with our prototype filter is well within the required range and is much narrower than the passbands commonly used in submillimeter photometry. The ability to change λ and $\Delta\lambda/\lambda$ also permits selection of passbands which avoid strong atmospheric absorption bands and hence may permit reductions in sky noise.

II. CONSTRUCTION

Figure 1 shows the assembly of an individual reflecting element.

Figure 2 shows the assembly of the three reflecting elements and the various spacers. The assembled filter has withstood many temperature cycles between 300 K and 1 K. It has also withstood inadvertent acceleration tests between lab bench and floor. It has been dismantled and reassembled with no detectable change in the transmission spectrum.

III. TUNING: PERFORMANCE

Each half of a double half wave filter (DHW) is a Fabry-Perot (FP). The filter is tuned by first tuning each FP separately.

The DHW is analogous to a transmission line (the optical path in free space) into which two resonant structures (the FP's) are inserted in parallel.[3,4] As is well known, such an arrangement results in higher transmission and a more nearly square passband than for either of the single resonant structures alone.

The passband of the assembled DHW filter is shown in Figure 3. As shown here the tuning is not yet optimized with respect to displacement from strong atmospheric absorption lines.

The work on this filter has been supported by a consortium agreement NCA2-OR108-200 between the University of Chicago and NASA-Ames Research Center.

A paper describing the filter in greater detail will be prepared when all tests are completed.

REFERENCES

[1]Ulrich, R., K. F. Renk, and L. Genzel, "Tunable Submm Interferometers of the FP type." I.E.E.E. Trans. on Microwave Theory and Techniques 11, 363-71 (1963).

[2]Holah, G. D., B. Davis, and N. D. Morrison, "Narrow-Bandpass Filters for the FIR using DHW Designs." I.R. Physics 19, 639-47 (1979).

[3]Macleod, H. A. Thin Film Optical Filters. New York: American Elsevier Publishing Company, 1969. P. 172.

[4]Born, M. and E. Wolf. Principles of Optics. Pergamon Press, 1980. P. 323.

[5]Whitcomb, S. and J. Keene, "LP Interference Filters for Submm Astro." Applied Optics 19, 197 (1980).

TABLE I

CHARACTERISTICS OF PROTOTYPE DOUBLE HALF WAVE FILTER

λ_0	286 μm
$\Delta\lambda/\lambda_0$	0.16
grid spacing	150 μm
grid period:	
center reflector	50 μm
end reflectors	150 μm
grid type:	
Buckbee-Mears Co electroformed nickel mesh flashed with gold	

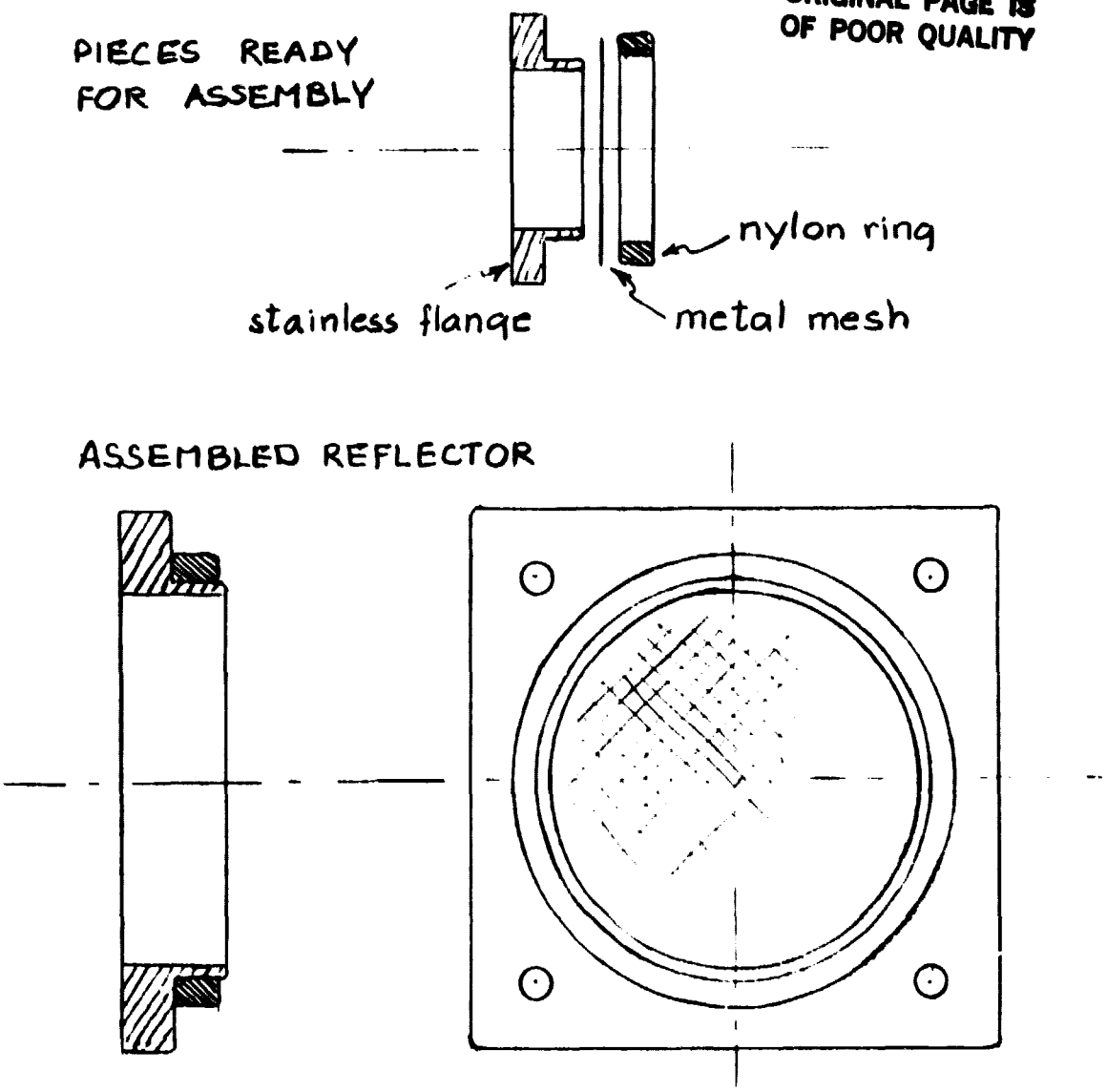

FIGURE 1. Assembly of an Individual Reflecting Element. The nylon ring is forced over the snout of the stainless flange, thus folding the edges of the metal mesh around the snout and pressing them tightly against the stainless surface. The coefficients of thermal expansion of the materials are such that the mesh is more tightly clamped and stretched as the filter cools.

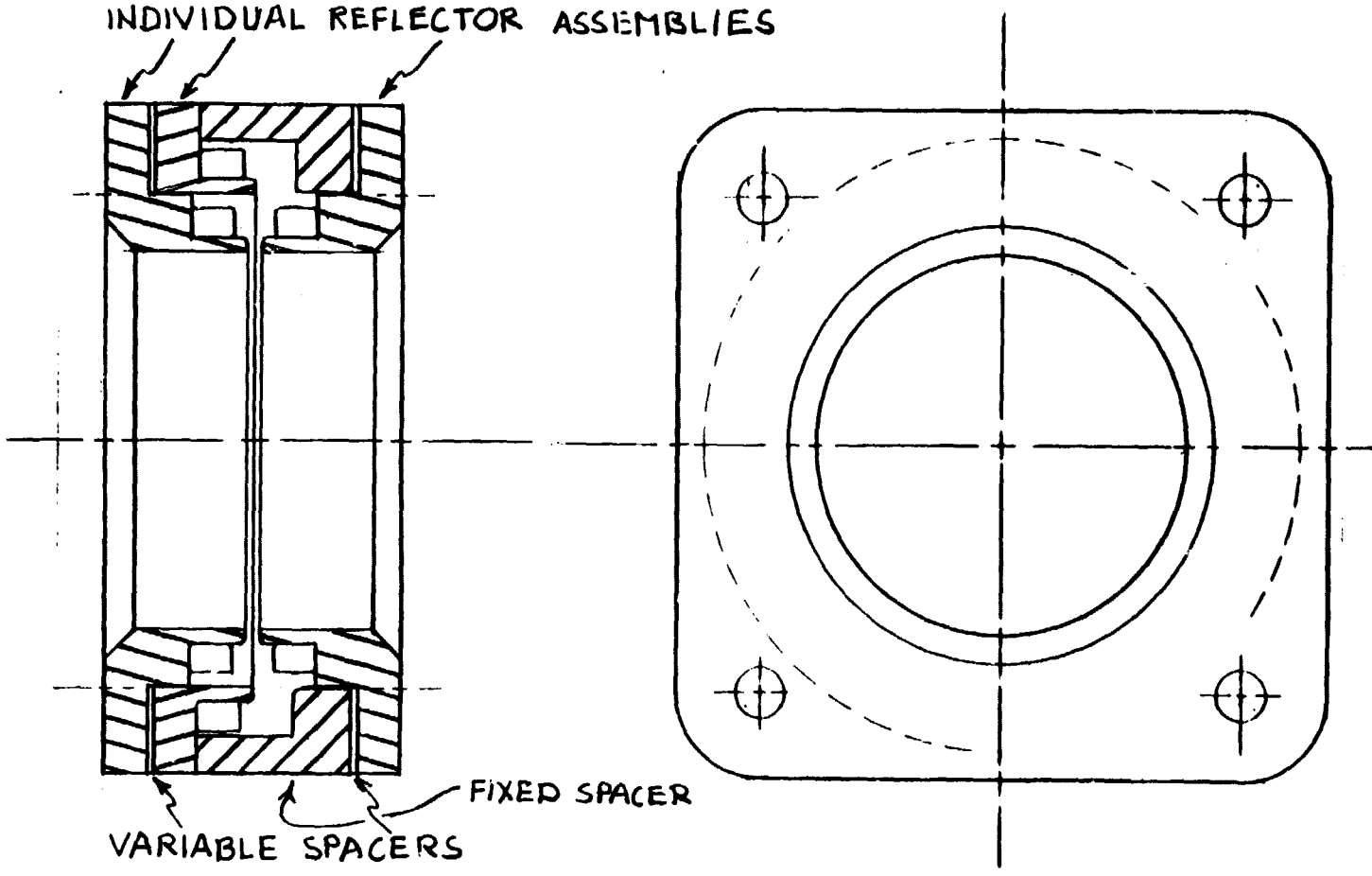

FIGURE 2. Assembly of Reflecting Elements and Spacers to Form the Double Half Wave Filter

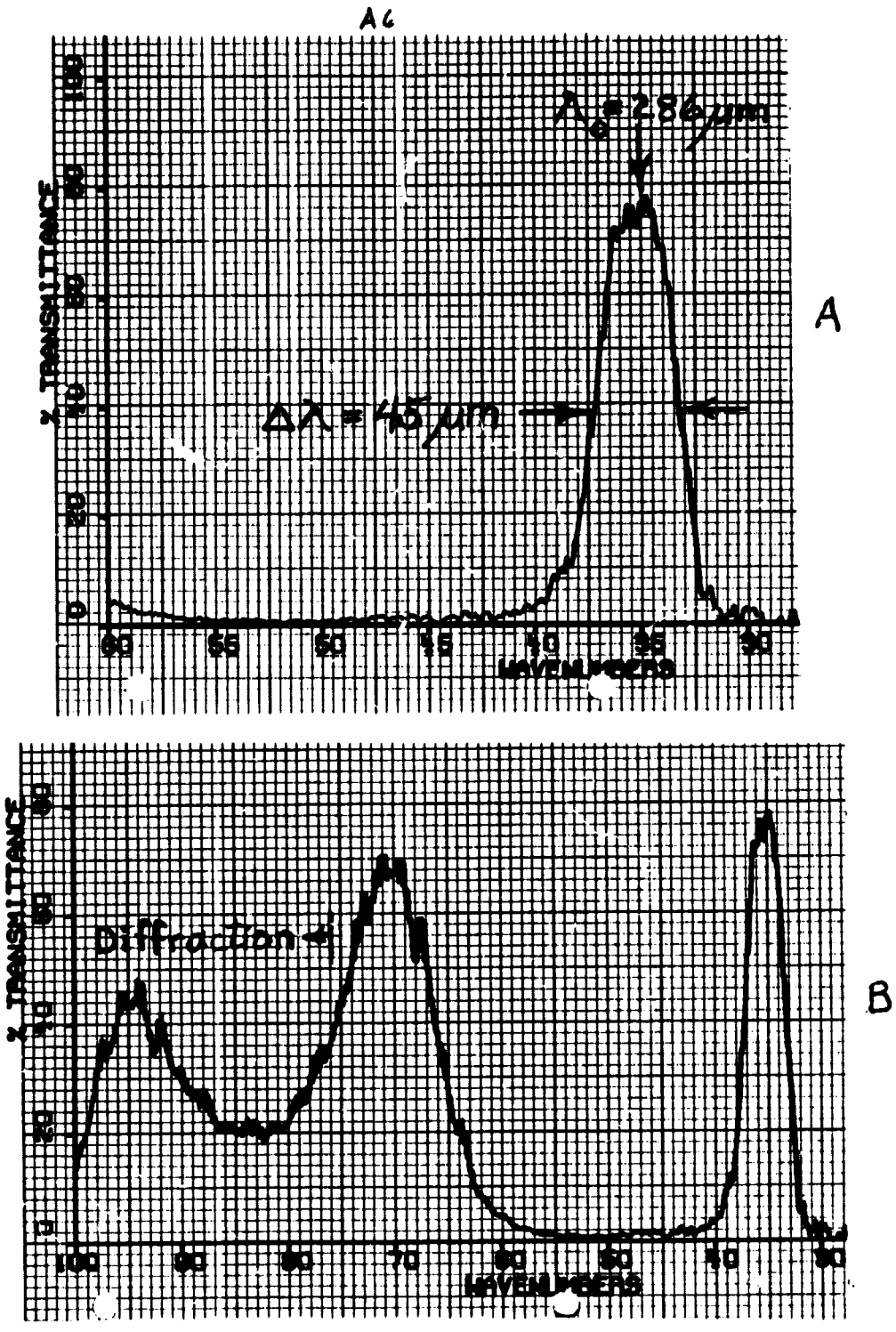

FIGURE 3. A. Passband of Double Half Wave Filter in Region of Interest

B. Passband over a Wider Range of Frequencies. Diffraction becomes dominant at wavenumbers greater than ~76 cm^{-1}. A low pass filter[5] is used to reject all but the fundamental passband.

APPENDIX B

Note: This DRAFT is still being checked by the authors. Please do not quote the results.

FAR-INFRARED DETECTION OF A LOW-LUMINOSITY PROTOSTAR IN THE BOK GLOBULE 335

Jocelyn Keene,[1,2,3] J. A Davidson,[2,3] D. A. Harper,[2] R. H. Hildebrand,[2,3]

D. T. Jaffe,[2,3,4] R. Loewenstein,[2] F. Low,[5] R. Pernic[2]

Subject headings: infrared: sources; nebulae: general; interstellar: matter

---

[1]California Institute of Technology

[2]University of Chicago

[3]Visiting Astronomer at the Infrared Telescope Facility, which is operated by the University of Hawaii under contract to the National Aeronautics and Space Administration

[4]Space Sciences Laboratory, University of California

[5]University of Arizona

FAR-INFRARED DETECTION OF A LOW-LUMINOSITY PROTOSTAR IN THE BOK GLOBULE 335

I. INTRODUCTION

B335 is a well-defined example of the type of isolated dust cloud identified by Bok as a "large globule" (Bok and Cordwell, 1973 and references therein). It is also the first such object to be detected in the far-infrared (Keene et al., 1980; hereinafter Paper I). The visually opaque region is ∿2' EW × 3' NS. Keene, Capps, and Whitcomb (1982) have recently shown that the central visual extinction is >40 mag. Based on the lack of foreground stars, Bok and McCarthy (1974) estimate that its distance is <400 pc.

The idea that stars may be condensing within globules was first proposed by Bok (1946). Martin and Barrett (1978) and Dickman (1978) studied the molecular line emission from globules and concluded that they are gravitationally bound and possibly contracting. Theoretical models by Kenyon and Starrfield (1979) and Villere and Black (1980) provide additional support for this hypothesis. However, others have argued (e.g., Herbig, 1974 and van den Bergh, 1972) that globules may be the dissipating remnants of larger clouds.

A recent survey of 9 globules by Keene (1981; hereinafter Paper II) concluded that their far-infrared surface brightnesses may be consistent with the hypothesis that they are heated only by the ambient interstellar radiation field (ISRF). She also noted that the mean surface brightness of B335 in a 1!7 beam was larger than that of the other objects by about a factor of two. Because of the uncertainty in the value of the ISRF, however, it was not clear that this required an additional source of heating.

The measurements presented here were made with higher spectral and spatial resolution than those of Papers I and II. They reveal that the

far-infrared source is much more compact than previously assumed, definitively ruling out the ISRF as a dominant heat source. The new far-infrared size, luminosity, and temperature which we derive suggest that we may be seeing the first direct evidence for a low-mass, pre-main-sequence star in a Bok globule.

II. OBSERVATIONS

We observed B335 with the NASA 3 m Infrared Telescope (IRTF) in February, 1981, and with the 0.9 m telescope of NASA's Kuiper Airborne Observatory (KAO) in October, 1981 and August, 1982.

The IRTF observations were made with the University of Chicago submillimeter photometer (Whitcomb, Hildebrand, and Keene, 1981) during a period of exceptionally clear and dry weather. We estimate that the precipitable water vapor at the zenith was 0.25 mm.

The KAO observations were made with the Yerkes Observatory "G-2" and "H-1" photometers. The G-2 photometer employs seven He^4-cooled germanium bolometric detectors arranged in a hexagonal array. The beams are 49" in diameter and are separated by 56". He-cooled filters provide a variety of spectral passbands. An aperture mask can be used to restrict the detectors' field of view to 33". In this system, the signal from the central detector can be subtracted from the average for the surrounding six detectors to eliminate correlated noise. The 60-μm measurements reported here were made using the 33" beams and the noise cancellation algorithm. The H-1 photometer is a new system employing a He^4-cooled germanium-diamond composite bolometer. It contains eight interchangeable apertures and eight interchangeable He^4-cooled filters. The apertures used in this work save fields of view of 42" and 87". The spectral passbands were set by a combination of two relfections from thallium bromide and transmission through various low- and high-pass metal mesh interference filters.

Observations and instrumental characteristics are summarized in Table 1. For the IRTF observations, the chopper throw was ' in the direction. For the KAO measurements, the chopper throw was 4' and the position angle was 100 (east from north).

III. RESULTS

(a) Source Size

Our spatial scans of B335 are displayed in Figure 1. For the 400 μm data, we have averaged the signals for the two sets of four data points taken at positions offset from the center by 30" and 60" in the NS and EW directions in order to increase the signal-to-noise ratio. The solid lines shown in the figure are scans of Mars made on the same nights as the B335 scans in order to establish the instrumental profile. The multi-aperture measurements at 110 and 140 μm and the 110 μm and 400 μm scans indicate that B335 is dominated by a single compact component. The half-power width of the 210 μm scan is ∿15% larger than the 90" beamwidth of the Mars scan. However, the Mars scan is incomplete, and the effective wavelength of the broad filter used in the observations is ∿30 μm longer for B335 than for Mars. From observations of other globules (Paper II), we would expect a flux density of about 30% of the observed value if there were no internal heating source. We estimate that the compact "core" source is <30" in diameter and accounts for >50% of the total far-infrared flux. This size is much smaller than the globule's apparent optical size and its extent in CO emission (see Plate 1). The position of the compact source as determined from the 110 μm and 400 μm scans is $19^h\ 34^m\ 34\overset{s}{.}7$, +7° 27' 20" (1950).

(b) Temperature

The source spectrum is displayed in Figure 2. Longward of 110 μm, the solid line has the form $\nu^2 B(\nu, T)$ with $T = 15$ K. Shortward of 110 μm,

it has the form $\nu^{-2.5}$. The dashed line is proportional to $\nu B(\nu, T)$ with T = 19 K. Lowering the 200 μm flux density (e.g., by subtracting the contribution to the large-aperture fluxes from an extended "halo") would broaden the spectrum, but it would still drop rapidly longward of 250 μm and shortward of 100 μm. The net effect would be to require contributions to the observed spectrum from dust at somewhat less and somewhat greater temperatures than derived from the curve in Figure 2. The 60 μm data require the presence of some dust grains at temperatures of >25-30 K. Refinement of these estimates must await better information on the spatial structure of the source and photometry at shorter wavelengths.

(c) Luminosity and Surface Brightness

The integrated flux from B335 (measured under the solid curve in Figure 2) is 1.6×10^{-12} W m^{-2}. This is slightly larger than the value quoted in Paper I. The difference stems primarily from the improved short-wavelength data. The coresponding source luminosity is 7.6 (D/400 pc) $L_\odot$.

Because the measured source size is much smaller than assumed in Paper I (based on the optical size of the cloud), the derived surface brightness is much higher. If the source is a uniform disk with a diameter of 30", the intensity is 10^{-4} W m^{-2} sr^{-1}, an increase of about a factor of 16. This definitively rules out heating by the ISRF, which has an intensity of only 1.8×10^{-8} W m^{-2} sr^{-1} (Werner and Salpeter; see discussion in Paper II).

(d) Comparison with B361

We also re-observed B361 on the same KAO flight on which we obtained our new long-wavelength data on B335. In agreement with the results of Paper II, its size in the far-infarared appears to be comparable to its extent in optical extinction and CO emission. It also appears to have a

lower temperature than B335; the ratio of its 140 μm to 190 μm flux densities (0.19) is lower than that of B335 (0.42), suggesting a value of perhaps 13 K rather than 15 K. Further observations will be needed to determine "typical" spectra for clouds with and without internal heating.

IV. NATURE OF THE CENTRAL SOURCE

(a) Mass, Density, and Extinction

The central emission peak in B335 represents a sharp peak in dust column density as demonstrated by the sharpness of the intensity peak in the 400 μm spatial scan. Flux densities at 400 μm are less sensitive to differences in temperature than those at shorter wavelengths. The sharp density peak is also seen in the near-infrared extinction data of Keene, Capps, and Whitcomb (1982).

We can estimate the amount of mass in the central region of B335 from the 400 μm optical depth. The flux density at 400 μm is 20 ± 2 Jy into a 48" beam. The source size, however, is smaller than the beam; an estimate of 30" appears to be consistent with the 210 and 400 μm scans. This corresponds to an average optical detph of 0.02 in a 30" diameter region for T = 15 K. We use the relationship between 400 μm optical depth and hydrogen column density derived by Keene, Hildebrand, and Whitcomb (1982; see also Hildebrand, 1983) to estimate the column density and thus the mass of the central condensation.[1] We find a total mass of 6.5 $M_\odot$ and an H_2 column density of 1.2×10^{23} cm^{-2}. For a uniform spherical source of 30" diameter, this column density implies a volume H_2 density of 1.0×10^6 cm^{-3}. The optical depth measurement also leads to an estimate for

[1]Estimates of column density, mass, volume density, and extinction are linearly proportional to the 400 μm optical depth. For these estimates we use $\tau_{400} = .025$, which was derived for T = 15 K. The corresponding values for T = 19 K are smaller by a factor of 0.56.

the visual extinction of $A_V \approx 123$.

The density, column density, and extinction inferred from the 400 μm data are much larger than those inferred from molecular line measurements (Dickman, 1978; Martin and Barrett, 1978). It is likely that much of the discrepancy is due to saturation of ^{13}CO lines in the cloud center, despite the approximate agreement of $C^{18}O$ column densities (Keene and Jaffe, 1982) with the ^{13}CO densities of Martin and Barrett (1978, measured with a 1' beam), to inaccuracies in the assumed gas and dust temperatures, and to the assumption of isothermal source structure.

(b) Luminosity and Age

Our measured total flux and the distance estimate, ≤400 pc, by Bok and McCarthy (1974) yield an upper limit of 6.4 $L_\odot$ for the total luminosity of the embedded compact object powering B335.

We do not believe that gravitational contraction can account for the luminosity of the core of B335. In Paper I we approximated the energy released by contraction as being the gravitational potential energy divided by the time scale for contraction, or

$$L_\odot \sim \left(\frac{GM^2}{\tau}\right) / \left(\frac{2\tau}{\Delta v}\right) ,$$

where M is the mass of the cloud, τ is the radius, and Δv is the measured velocity width of molecular lines. We concluded that gravitational contraction could produce only 0.009 $L_\odot$. We can revise that estimate now, using new values for the mass, radius, and velocity: $M = 6.5\ M_\odot$, $\tau = 9 \times 10^{16}$ cm, and $\Delta v = 2$ km s^{-1}. The new result is ∿0.1 $L_\odot$, still much less than the observed luminosity. It would be possible to produce the observed luminosity only if there were a much greater mass of material hidden in the center of the cloud. This would of course be possible if the core were optically thick to submillimeter radiation. However, a compact

object with that mass would probably have a very high luminosity (

If the embedded power source were a single main-sequence star, this would imply a spectral type of ∿F0 and a mass of ∿1.7 $M_\odot$. However, the time scale for the pre-main-sequence evolution of a low-mass star is long (>10^7 to 10^8 yr). If the star lies between the bottom of the Hayashi track and the main sequence, it could be slightly more massive for the same bolometric luminosity. If it is still descending the Hayashi track, it could be significantly less massive.

From the CO line profiles, Frerking and Langer (1982) conclude that there is a high velocity flow in B335. They argue that this can best be explained by mass loss at a rate of 10^{-8} $M_\odot$/yr from a protostellar object within the cloud. This flow resembles those seen in other regions believed to surround pre-main-sequence objects (Bally and Lada, 1983) except that the far-infrared data show this one to be much less energetic. A lower limit for the age of the source can be derived from the dynamical "age" of the high velocity flow. Taking its extent to be 2.5 and its velocity to be 3 km/s (Frerking and Langer, 1982), its lifetime is $l/v = 10^5$ yr.

In summary, we have detected a compact far-infrared source in the center of B335. Its luminosity implies that the exciting star has a mass of <2 $M_\odot$. The source provides the best evidence to date for star formation in an isolated Bok globule.

ACKNOWLEDGEMENTS

We thank the staffs of the KAO and IRTF for their expert technical support. The airborne observations were supported by NASA grants NSG-2057 and NGR-14-001-227; the IRTF observations by NASA grant NAG-W-4.

REFERENCES

Bally, J. and Lada, C. J. 1983, *Ap. J.*, in press.

Bohlin, R. C. Savage, B. D., and Drake, J. F. 1978, *Ap. J.* 224, 132.

Bok, B. J. and Cordwell, C. S. 1973, in *Molecules in the Galactic Environment*, M. A. Gordon and L. F. Snyders, eds. (New York: Interscience), p. 54.

Bok, B. J. and McCarthy, C. C. 1974, *A. J.* 79, 42.

Dickman, R. L. 1978, *Ap. J. Suppl.* 37, 407.

Frerking, M. A. and Langer W. D. 1982, *Ap. J.* 256, 523.

Herbig 1974, *P.A.S.P.* 86, 604.

Keene, J. 1981, *Ap. J.* 245, 115

Keene, J., Capps, R. W., and Whitcomb, S. E. 1982, in preparation.

Keene, J., Harper, D. A., Hildebrand, R. H., and Whitcomb, S. E. 1980, *Ap. J. (Letters)* 240, L43.

Keene, J. Hildbrand, R. H., and Whitcomb, S. E. 1982, *Ap. J. (Letters)* 252, L11.

Keene, J. and Jaffe, D. 1982, unpublished.

Kenyon, S. and Starrfield, S. 1979, *P.A.S.P.* 91, 271.

Martin, R. N. and Barrett, A. H. 1978, *Ap. J. Suppl.* 36, 1.

van den Bergh, S. 1372, *Vistas in Astronomy* 13, 265.

Villere, K. R. and Black, D. C. 1980, *Ap. J.* 236, 192.

Whitcomb, S. E. and Keene, J. 1980, *Appl. Optics* 19, 197.

Whitcomb, S. E., Hildebrand, R. H., and Keene, J. 1980, *P.A.S.P.* 92, 863.

TABLE 1

Summary of Observations

Observatory	Passband (μm)	Mean Wavelength (μm)	Beam Diameter (arc sec)	Flux Density (Jy)	Errors		Calibration Object
					Stat.	Total	
KAO	45-80	60	33	7	1	2	W3(OH)
	85-120	110	42	35	5	9	W3(OH)
	85-120	110	90	34	8	11	W3(OH)
	130-150	140	42	38	5	9	W3(OH)
	130-150	140	90	45	5	10	W3(OH)
	125-150	140	102	33	12	13	W51
	150-200	180	90	80	8	18	W3(OH)
	160-230	190	102	84	17	24	W51
	160-300	200	90	67	3	14	W3(OH)
	160-1000	235	102	61	7	14	W51
MKO	300-900	400	48	19	2	4	W51
	520-2000	1000	102	1.8	0.6	0.7	W51

Fig. 1. Scans of B335 compared to scans of Mars at three wavelengths. The beam diameter in arc sec. is shown below the effective wavelength in each panel. The solid lines are the Mars scans (asymmetrical at 110 μm and 210 μm when the scan is in the chopping direction). At 210 μm we show the data for a north-south scan (closed circles) and an east-west scan (open circles) in the same panel. The Mars curve at 210 μm is from a single east-west scan.

Fig. 2. Source Spectrum of B335. The symbols identify the measurements and beam sizes. The dashed curve has the form $\nu B(\nu, 19K)$. Longward of 110 μm the dark solid line has the form $\nu^2 B(\nu, 15K)$ and shortward of 110 μm it has the form $\nu^{2.5}$. The light solid line shortward of 110 μm has the form $\nu^2 B(\nu, 15K)$.

Fig. 3. The Bok Globule B335. The photograph is from the National Geographic Society-Palomar Observatory Sky Survey. The position of the unresolved far IR/submillimeter source [$\alpha(1950) = 19^h34^m34^s.7$, $\delta(1950) = +7°27'20''$] is shown by the cross at the center (reference point for offset scales). The dotted circle shows the half-power 400 μm beam width (48''). The solid contours show ^{13}CO ($J = 1 \rightarrow 0$) antenna temperatures (Martin and Barrett, 1978) at intervals of 0.5 K with a peak value of 3.5 K at the innermost contour. The half-power ^{13}CO beam width (1!1) is shown at the upper left.

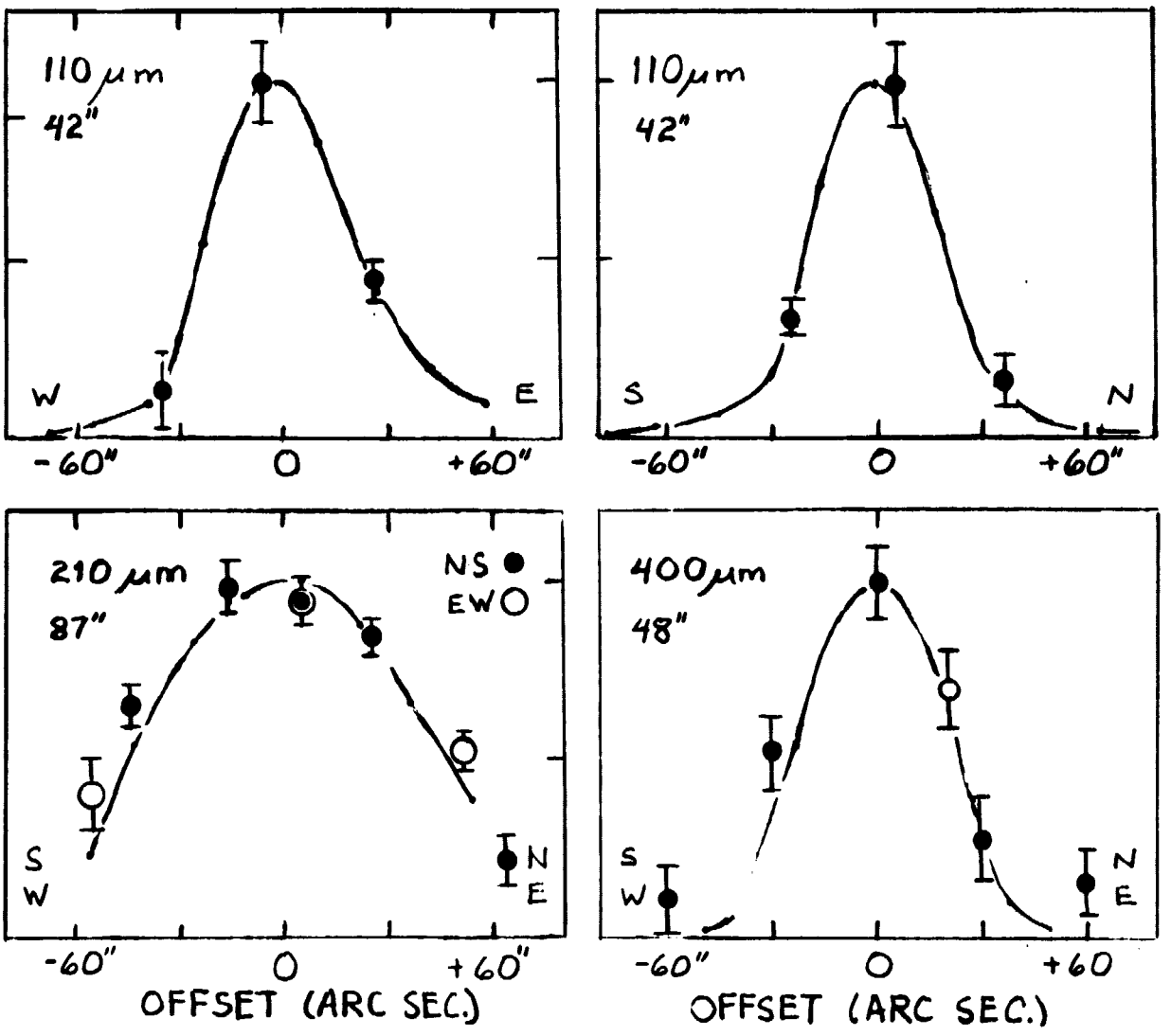

FIG 1

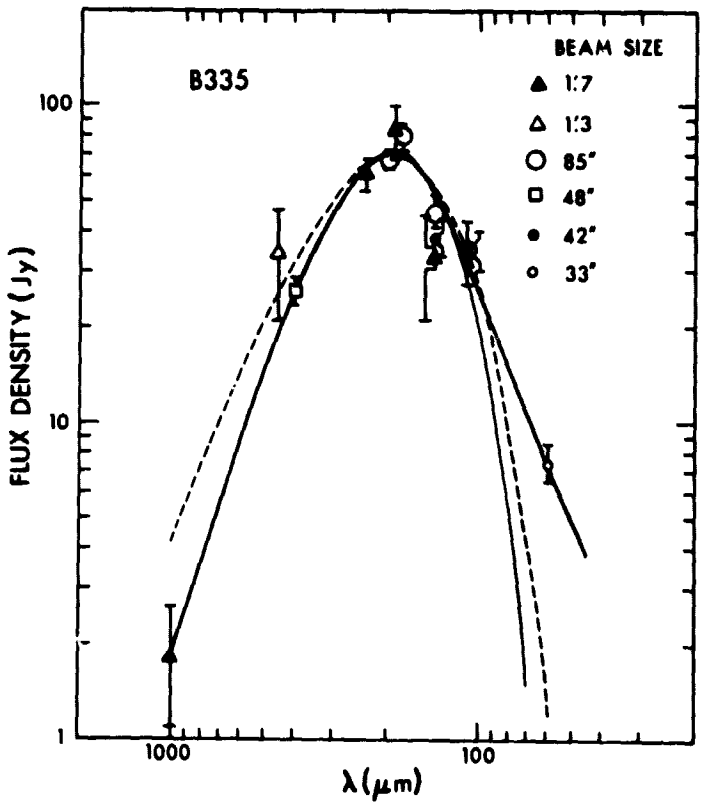

Fig. 2

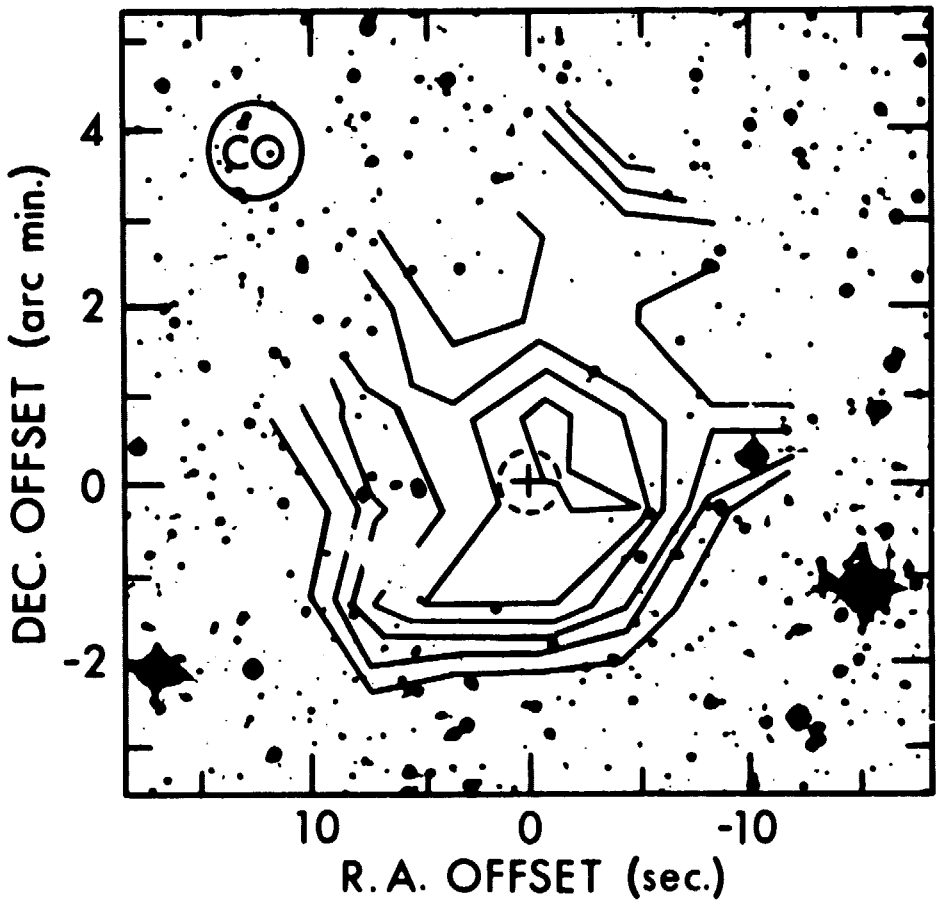

Fig.3